

AD-A104 315 FOREIGN TECHNOLOGY DIV WRIGHT-PATTERSON AFB OH
HOLOGRAPHIC PROCESSING OF PULSED DOPPLER RADAR. (U)
AUG 81

F/G 17/9

UNCLASSIFIED FTD-ID(RS)T-1905-80

NL

| or |
AD A
102316

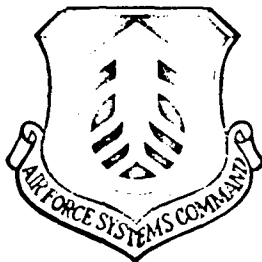
END
DATE
FILED
10-81
DTIC

AD A104315

FTD-ID(RS)T-1905-80

(2)

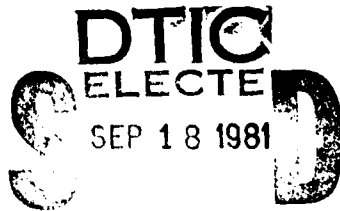
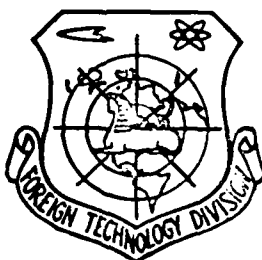
FOREIGN TECHNOLOGY DIVISION



HOLOGRAPHIC PROCESSING OF PULSED DOPPLER RADAR

by

Chinese Academy of Sciences, Institute of Physics
Optical Information Processing Group



Approved for public release;
distribution unlimited.



81 9 18 7

DTIC FILE COPY

FTD-ID(RS)T-1905-80

EDITED TRANSLATION

FTD-ID(RS)T-1905-80

27 August 1981

MICROFICHE NR: FTD-81-C-000786

HOLOGRAPHIC PROCESSING OF PULSED DOPPLER RADAR

By: Chinese Academy of Sciences, Institute of
Physics, Optical Information Processing
Group

English pages: 22

Chinese Academy of Sciences, Institute
of Physics 25-35

Country of origin: China

Translated by: SCIFRAN

F33657-78-D-0619

Requester: FTD/TQTA

Approved for public release; distribution
unlimited.

THIS TRANSLATION IS A RENDITION OF THE ORIGINAL FOREIGN TEXT WITHOUT ANY ANALYTICAL OR EDITORIAL COMMENT. STATEMENTS OR THEORIES ADVOCATED OR IMPLIED ARE THOSE OF THE SOURCE AND DO NOT NECESSARILY REFLECT THE POSITION OR OPINION OF THE FOREIGN TECHNOLOGY DIVISION.

PREPARED BY:

TRANSLATION DIVISION
FOREIGN TECHNOLOGY DIVISION
WP-AFB, OHIO.

FTD-ID(RS)T-1905-80

Date 27 Aug 1981

1410 8/11

EXPERIMENTAL RESEARCH

Holographic Processing of Pulsed Doppler Radar

by

Chinese Academy of Sciences, Institute of Physics
Optical Information Processing Group

| | |
|--------------------------------------|---------|
| Accession For | |
| NTIS GRA&I | |
| DTIC TAB | |
| Unannounced <input type="checkbox"/> | |
| Justification | |
| By _____ | |
| Distr. (Line) | |
| Availability Codes | |
| Avail. and/or | |
| Distr | Special |

X

I. INTRODUCTION

The storage and reconstruction of an electric signal is extremely easy using modern electronic equipment such as an oscilloscope or a magnetic tape recorder. Arm and King ⁽¹⁾ used a holographic technique to optically record and reconstruct electric signals and attempted to process radar signals ⁽²⁾ using this method. It may appear to most people that the holographic method is far more complicated than electronic techniques. However, as we are going to discuss here, the holographic technique has many advantages over other methods, including two-dimensional resolution capability, capacity, speed, and simplicity in instrumentation. The principle of this holographic technique is schematically shown in Figure 1.

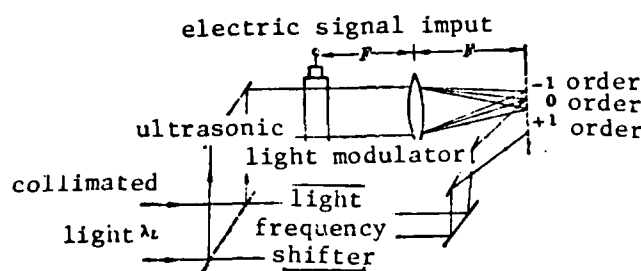


Figure 1.

An electrical input signal is converted to a one-dimensional

spatial transmittance function by an ultrasonic light modulator (which acts as a moving phase grating). The modulated light beam carries two fringes with information on the input electric signal. It then undergoes a Fourier transform to the back focal plane of the cylindrical lens and forms one zero order and two first order lines. The ± 1 order fringes are symmetrical with respect to the zero order line. It is then possible to form a Fourier hologram using either one of the first order fringes and a plane reference beam through interference. The hologram records and stores all the information carried by the electric signal, including frequency, amplitude, and phase. The reconstruction of the electric signal can be achieved using a reverse Fourier transform. The reference beam is generated using the partial compensation method originally proposed by Arm and King. This method uses an ultrasonic light modulator, which is driven with a continuous signal in the reference beam. Therefore, the frequency of the reference beam shifts as the recording of the frequency of the electric input signal is completed. This arrangement allows a steady interference pattern over longer exposure time for the hologram. Consequently, the power and bandwidth requirements of the laser can be lowered.

Pulse Doppler radar emits a train of pulses with fixed phase relation. It is then possible to detect the velocity of the target based on the phase changes of the return signals. The resolution of the Doppler radar, of course, depends on the observation time of the target. For high resolution, it requires the gathering of many return signals which can be easily processed using the optical technique. Once the motion of the film coincides with the repetition frequency of the radar, one can record the holograms of the return signals of all the targets. These holograms still contain the phase relation of all the return signals which, upon reconstruction with a spherical lens, provides a two-dimensional capability to show distance and

velocity of the targets. Such capabilities are still not possible using modern electronic systems.

This paper briefly introduces the partial compensation methods originated by Arm and King with emphasis on the theory of the two dimensional (distance - velocity) capability of the radar system. It also shows some experimental results using simulated signals. Finally, an evaluation and a projection of the role of optical holographic processing methods used in pulsed Doppler radar are given.

Theory

1. Fourier Transform Characteristics (Thin Lens)

The basic principle of the holographic processing technique is based on the following Fourier transform which describes the optical amplitude distributions at the front and back focal planes of an ideal thin lens

$$B(x', y') = K' \int_{-P/2}^{+P/2} \int_{-P/2}^{+P/2} G(x, y) \exp\left[-j \frac{2\pi}{F\lambda_L} (xx' + yy')\right] dx dy \quad (1)$$

where K' is a constant, $K' = (j/F\lambda_L) e^{j\frac{2\pi P}{\lambda_L}}$, λ_L is the wavelength, F is the focal length. Equation (1) is valid only when $P \ll F$ and $P' \ll F$.

If a cylindrical lens is used instead of a spherical lens, then the two dimensional Fourier transform becomes one-dimensional:

$$B(x') = K \int_{-P/2}^{+P/2} G(x) \exp\left(-j \frac{2\pi}{F\lambda_L} xx'\right) dx \quad (2)$$

where $K = K'^{1/2}$, and the holographic processing system is schematically shown in Figure 2.

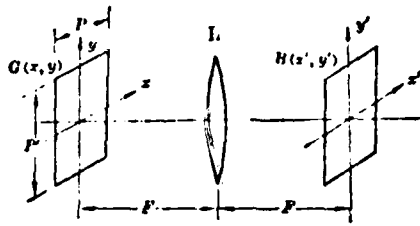


Figure 2.

2. Expression of Pulse Doppler Radar Return Signals

An electric signal can usually be expressed as:

$$v(t) = a(t) \cos[\omega t + \theta(t)] \quad (3)$$

where ω is the carrier frequency, $\theta(t)$ is the phase factor, $a(t)$ is the envelope of reflected amplitude change. The IF frequency of the i th return after the mixing of the pulsed Doppler returns can be expressed as:

$$v_i(t) = K_0 a_i [t - (i-1)T] \cos[(\omega_0 + \omega_d)t - \omega_d(i-1)T] \quad (4)$$

where ω_0 - phase factor, ω_0 - IF frequency
 ω_d - Doppler shift due to target movement
 $\omega_d = -\frac{2V}{c} \omega_0$, V - target radial velocity
 ω_c - carrier frequency of radar signal
 T - period of radar scanning
 K_0 - constant

The above equation does not contain any second or higher order terms. The terms $(\omega_0 + \omega_d)$ and $\omega_d(i-1)T$ represent the Doppler shift in frequency and phase of the return signals, respectively. This indicates that a moving target not only causes a frequency shift but also a phase change.

For convenience, the return signal can be expressed in complex number

$$v_i(t) = v_{ii}(t) + v_{ii}^*(t)$$

$$v_{ii}(t) = \frac{K_0}{2} a_r [t - (i-1)T] \exp\{j[(\omega_0 + \omega_d)t - \omega_d(i-1)T]\} \quad (5)$$

where

$$v_{ii}^*(t) = \frac{K_0}{2} a_r [t - (i-1)T] \exp\{-j[(\omega_0 + \omega_d)t - \omega_d(i-1)T]\}$$

They represent the two fringes of $v_i(t)$, and * represents the complex conjugate.

3. Ultrasonic Light Modulator

When an electric signal $v(t) = a(t) \cos[\omega t + \theta(t)]$ is received by the transducer of an ultrasonic light modulator, a pressure wave travelling at the speed of sound s is produced in the delay medium. According to Debye effect, the index of refraction of this medium changes as the pressure wave propagates which leads to a phase change of the light beam passing through such a medium. The changes are proportional to the input electric signal.

$$\psi(x, t) - \psi_0 = K_s v \left(t - \frac{x}{s} \right)$$

where K_s is the proportionally constant, ψ_0 is the phase transition of the medium in the absence of the pressure wave where $\psi(x, t)$ is the phase transition as the pressure wave propagates.

The transmittance of a transparent medium $T(x) = 1$. An ultrasonic light modulator can be considered as a phase modulator with transmittance function $T_s(x, t) = \exp[j\psi(x, t)]$ or

$$T_s(x, t) = F(x) \exp[j(\psi_0 + K_s v \left(t - \frac{x}{s} \right))] \quad (6)$$

where $F(x)$ is defined as the spatial pulse function (along x-direction)

$$F(x) = \begin{cases} 1 & \text{when } |x| < \frac{1}{2} P \\ 0 & \text{when } |x| > \frac{1}{2} P \end{cases}$$

where P is the optical path along x direction, P/s is the storage time of the ultrasonic light modulator.

Under normal conditions, to alleviate non-linear effects, it is usually operated under very little pressure. In this case, $K_s v \left(t - \frac{x}{s} \right)$ is small and

$$\exp jK_s v \left(t - \frac{x}{s} \right) \approx 1 + jK_s v \left(t - \frac{x}{s} \right)$$

The transmittance of the ultrasonic light modulator can be written as:

$$T_s(x, t) = F(x) \exp j\psi_0 + jF(x) K_s v \left(t - \frac{x}{s} \right) \exp j\psi_0 \quad (7)$$

The optical amplitude after spatial modulation is:

$$G(x, t) = G_p T_s(x, t) = G_p F(x) \exp j\psi_0 + G_p jF(x) K_s v \left(t - \frac{x}{s} \right) \exp j\psi_0 \quad (8)$$

In (8), G_p is the plane wave front. The first term is a constant, representing the fixed optical phase shift due to the modulator, or zero order light. The second term contains the electric signal $v(t)$ and can be expressed as

$$v \left(t - \frac{x}{s} \right) = v_1 \left(t - \frac{x}{s} \right) + v_1^* \left(t - \frac{x}{s} \right),$$

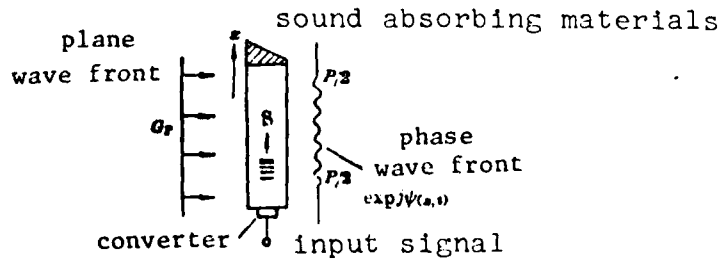


Figure 3

$v_1(t - \frac{x}{s})$ and $v_1(t - \frac{x}{s})$ are the two fringes. The ultrasonic light modulator can be considered as a phase grating moving at speed s . A light beam forms two first order fringes, when passing through the grating, corresponding to $v_1(t - \frac{x}{s})$ and $v_1(t - \frac{x}{s})$.

4. Fourier Frequency Spectral Analysis of $G(x, t)$

It is possible to use Fourier transform characteristics of the lens to obtain the one-dimensional spatial frequency spectrum $B(x', t)$ of $G(x, t)$ at the back focal plane by placing the ultrasonic light modulator at the front focus of the lens:

$$B(x', t) = K \int_{-p/2}^{+p/2} G(x, t) \exp j\left(-\frac{2\pi}{F\lambda_L} xx'\right) dx \quad (9)$$

As discussed earlier, $B(x', t)$ contains one zero order and two first order spectral lines corresponding to the zero order and two first order waveforms of $G(x, t)$ and the electric signal is only carried by the ± 1 lines.

Let's consider one of the first order fringes. Its optical amplitude can be expressed as:

$$B_1(x', t) = K_1 \int_{-p/2}^{p/2} v_1\left(t - \frac{x}{s}\right) \exp\left(-j \frac{2\pi}{F\lambda_L} xx'\right) dx \quad (10)$$

where $K_1 = jKG_F F(x)K_s \exp j\psi_0$, $v_1\left(t - \frac{x}{s}\right)$ = a constant and is one of the fringes of $v\left(t - \frac{x}{s}\right)$.

Considering that the recording time is far less than the storage time of the ultrasonic light modulator;

$$B_1(x', t) = K_1 \exp\left(-j \frac{2\pi}{F\lambda_L} xx't\right) A(x', 0) \exp[j\phi(x', 0)] \quad (11)$$

where

$$A(x', 0) \exp[j\phi(x', 0)] = \int_{-p/2}^{+p/2} v_1\left(-\frac{x}{s}\right) \exp\left(-j \frac{2\pi}{F\lambda_L} xx'\right) dx \quad (12)$$

is the amplitude and phase of the first order spectral line. From (11) we notice that the amplitude of the first order spectral line is independent of time with the exception of a factor $\exp(-j\frac{2\pi}{F\lambda_L}sx't)$. This time factor shifts the light frequency with amplitude $A(x', 0)$ by $\frac{x's}{F\lambda_L}$ (Hz) as x' changes.

5. Holographic Recording Using a Partial Compensation Method

Arm and Kind proposed the use of a partially compensating method to alleviate the instability of the interference pattern of a hologram due to the time dependent factor $\exp(-j\frac{2\pi}{F\lambda_L}sx't)$

It actually involved the use of an ultrasonic light modulator driven by a continuous signal in the reference beam. It caused a frequency shift of $\omega_0/2\pi$ in the plane reference beam and ω_0 is the median frequency of the return signal. The reference beam can then be written:

$$R(x', t) = R_0 \exp \left[j \left(\frac{2\pi}{\lambda_L} \right) \sin \alpha x' \right] \exp [j\omega_0 t] \quad (13)$$

where R_0 is a constant and it represents the amplitude of the reference beam. The first exponent indicates that the plane wave is incident upon the hologram at an angle α . The second exponent shows that the plane wave has a time dependent phase factor to compensate for the time-dependent factor in $B_1(x', t)$

The intensity distribution of the two interfering light beams can be expressed as: $I(x', t) = |R(x', t) + B_1(x', t)|^2$

$$= R_0^2 + 2R_0 K_1 A(x', 0) \cos \left[2\pi \left(\frac{x'}{\lambda_s} \right) - \phi(x', 0) + \omega_0 t + \left(\frac{2\pi}{F\lambda_L} x' st \right) \right]. \quad (14)$$

where $\lambda_s = \lambda_L / \sin \alpha$ is the carrier wavelength of the interference pattern. For linear recording results, it is already assumed in

the above equation that $R_0^2 \ll [K_1 A(x_0, 0)]^2$, i.e. the reference beam is far more intense than the signal beam.

The total exposure of the film is

$$E(x') = \int_{-T_0/2}^{T_0/2} I(x', t) dt \quad (15)$$

where T_0 is the exposure time.

$$E(x') = T_0 \left\{ R_0^2 + 2R_0 K_1 A(x', 0) \frac{\sin\left(\frac{T_0}{2}\right)\left(\omega_0 + \frac{2\pi}{F\lambda_L} x's\right)}{\frac{T_0}{2}\left(\omega_0 + \frac{2\pi}{F\lambda_L} x's\right)} \cdot \cos\left[2\pi\left(\frac{x'}{\lambda_s}\right) - \phi(x', 0)\right] \right\} \quad (16)$$

From equation (16), the film exposure decreases according to a $\sin u/u$ relation after partial compensation. At median frequency $\omega_0/2\pi$, the interference pattern is absolutely stable due to the perfect match between the signal beam and the reference beam. However, a loss in exposure due to the mismatch of the reference frequency at x' away from the median frequency will appear. If the median frequency of the input signal is $\omega_0/2\pi$ and the bandwidth is B_s , the largest exposure loss factor is

$$\sin\left(\frac{\pi B_s T_0}{2}\right) / \left(\frac{\pi B_s T_0}{2}\right)$$

When $T_0 < 2B_s$, the distortion becomes small. Therefore, the maximum value of T_0 depends on B_s as well as the resolution required.

6. Holographic Recording of N Radar Return Signals

Equation (16) represents the hologram of a single radar return signal. If the film moves in the spectrum line direction (y' direction as shown in Figure 4) on the (x', y') plane, it is possible to record multiple holograms of radar returns and the combined holograms can be expressed as:

$$E(x', y') = \sum_{i=1}^N E_i(x') F_i(y') \quad (17)$$

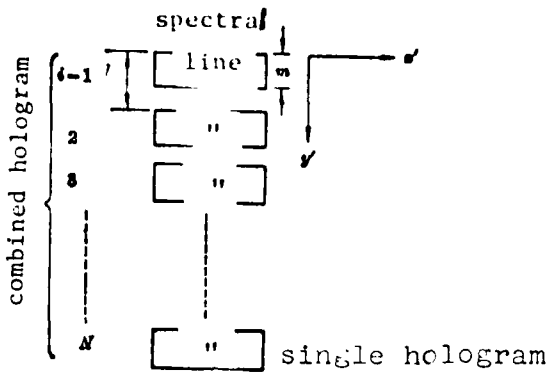


Figure 4

where $E_i(x')$ is the holographic expression of the i^{th} return signal and $F_i(y')$ is defined as a pulse function in the y' direction as:

$$F_i(y') = \begin{cases} 0 & l(i-1) + m < y' < l_i \\ 1 & l(i-1) \leq y' \leq l(i-1) + m \end{cases}$$

where l is the space between holograms and m is the width of the hologram.

Plugging (16) into (17), we get the exposure of holograms:

$$E(x', y') = \sum_{i=1}^N T_0 \left\{ R_0^2 + 2R_0 K_1 A_i(x', 0) \frac{\sin\left(\frac{T_0}{2}\right) \left[\omega_0 - \frac{2\pi x' s}{F \lambda_L} \right]}{\left(\frac{T_0}{2}\right) \left(\omega_0 - \frac{2\pi x' s}{F \lambda_L} \right)} \cdot \cos\left[2\pi\left(\frac{x'}{\lambda_s}\right) - \phi_i(x' 0)\right] \right\} \cdot F_i(y') \quad (18)$$

7. The Reconstruction of the Combined Hologram

As shown schematically in Figure 5 the reconstruction of the N^{th} hologram can be accomplished by placing the combined hologram at the front focal plane of a spherical lens using an opti-

cal slit (along y') as the control. Upon illumination by plane light, the two dimensional display of target distance-velocity can be obtained at the back focal plane.

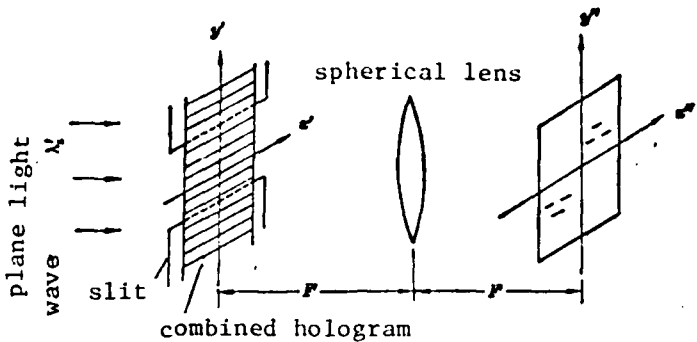


Figure 5. Reconstruction Scheme

For ease of calculation, equation (18) is simplified. The factor $\sin u/u$ is caused by the partial compensation which reflects the loss in intensity of the interference pattern of the hologram. It does not affect the principle of two dimensional display of signals. Therefore, this factor is going to be dropped from the following reasoning and equation (18) can be rewritten as

$$E(x', y') = \sum_{i=1}^N T_i \left\{ R_0^2 + 2R_0 K_1 A_i(x', 0) \cos \left[2\pi \left(\frac{x'}{\lambda_0} \right) - \phi_i(x', 0) \right] \right\} F_i(y') \quad (19)$$

Assuming that the film remains in the linear region of the H-D curve, then the transmittance of the hologram is proportional to the exposure $E'(x', y')$. Now that a plane wave G'_p is used to reconstruct the signal, then the optical amplitude $E_r(x', y')$ of light transmitted through the hologram is $\sim G'_p \cdot E(x', y')$

$$E_r(x', y') = K_2 + 2K_3 \sum_{i=1}^N \left\{ A_i(x', 0) \cos \left[2\pi \left(\frac{x'}{\lambda_0} \right) - \phi_i(x', 0) \right] \right\} F_i(y') \quad (20)$$

where $K_2 = T_0 G' p R_0^2 N$; $K_3 = T_0 R_0 K_1 G' p$ are constants.

The two dimensional Fourier transform with a spherical lens results in the following optical amplitude distribution on the back focal plane:

$$B(x'', y'') = K \int_{-Q/2}^{Q/2} \int_{-Q'/2}^{Q'/2} E_T(x', y') \exp \left[-j \frac{2\pi}{F' \lambda_L} (x' x'' + y' y'') \right] dx' dy'$$

where λ_L' is the wavelength of the reconstruction light, F' is the focal length of the spherical lens, Q and Q' are the coordinates of the combined hologram on the x' , y' axes. (see Figure 5).

Putting $E_T(x', y')$ into the above equation we get the three intensity terms:

$$I(x'', y'') = |B(x'', y'')|^2 = I_0(x'', y'') + I_{+1}(x'', y'') + I_{-1}(x'', y'') \quad (21)$$

$$I_0(x'', y'') = K_4^2 \delta^2(x'') \delta^2(y'') \quad (22)$$

Here $K_4 = K K_3 (F' \lambda_L)^2$, $I_0(x'', y'')$ is the intensity of the zero order light spot which does not carry any signal and it appears at $x'' = y'' = 0$.

The second term $I_{+1}(x'', y'')$ is one of the information carrying fringes:

$$I_{+1}(x'', y'') = |B_{+1}(x'', y'')|^2 = K_5^2 a_r^2(t_0) \left(\frac{\sin \frac{2\pi y''}{F' \lambda_L} \cdot \frac{m}{2}}{\frac{2\pi y''}{F' \lambda_L}} \right)^2 \cdot \left(\frac{\sin \frac{N}{2} \left(\omega_d T - \frac{2\pi}{F' \lambda_L} y'' l \right)}{\sin \frac{1}{2} \left(\omega_d T - \frac{2\pi}{F' \lambda_L} y'' l \right)} \right)^2 \quad (23)$$

where $K_5 = K_0 K K_3 \lambda_L F_0$ is a constant.

From equation (23) one can see that $B_1(x'', y'')$ is proportional to the envelope of $v_{it}^*(t_0)$. The only difference is that the origin has shifted by a distance d .

Since $t_0 = \frac{F\lambda_L}{F'\lambda'_L} \left(\frac{d-x''}{s} \right)$, $F\lambda_L/F\lambda'_L$ is the magnifying factor

which equals to 1 when the same wavelength is used in reconstruction and recording of the signals and the same focal length spherical and cylindrical lenses are used in the process. In this case:

$$F\lambda_L/F'\lambda'_L = 1, t_0 = \frac{d-x''}{s},$$

The distance d from the origin is totally dependent on the angle of incidence of the reference beam:

$$d (= F'\lambda'_L \sin\alpha / \lambda_L)$$

Similarly we can derive that $I_{-1}(x'', y'')$ is the other information carrying fringe in equation (20) which can be expressed as:

$$\begin{aligned} I_{-1}(x'', y'') &= |B_{-1}(x'', y'')|^2 \\ &= K \frac{2}{3} a_r^2(t_0) \left(\frac{\sin \frac{2\pi y''}{F'\lambda'_L} \cdot \frac{m}{2}}{\frac{2\pi y''}{F'\lambda'_L}} \right)^2 \left[\sin \frac{N}{2} \left(-\omega_d T - \frac{2\pi}{F'\lambda'_L} y'' l \right) \right]^2 \\ &\quad \left[\sin \frac{1}{2} \left(-\omega_d T - \frac{2\pi}{F'\lambda'_L} y'' l \right) \right]^2 \end{aligned} \quad (24)$$

where $t_0 = \frac{F\lambda_L}{F'\lambda'_L} \left(\frac{d+x''}{s} \right)$ which indicates that the origin has shifted by $-d$. $B_{-1}(x'', y'')$ is also found to be proportion to the envelope of $(t_0)v_{it}$.

8. Discussion on the Characteristics of the Two Dimensional Display of Distance and Velocity

(1) Two symmetrical images (I_{+1} and I_{-1}) appear in the reconstruction, each shifts by d (or $-d$) from the origin.

(2) Both I_{+1} and I_{-1} are proportion to $a_1^2 \left(\frac{x''}{s} \right)^2$, i.e. the intensity of the reconstructed image is proportional to the square of the amplitude envelope of the input signal. This property can be used to obtain signals from targets under rotation.

(3) Because the x'' coordinate on the display plane is proportional to the coordinate of the input electric signal in the ultrasonic light modulator (i.e., proportional to the delay time of the targets), it is then possible to obtain the relative distance of the target in the x'' direction.

(4) Both equations (23) and (24) contain the factor $\left(\frac{\sin Nu}{\sin u} \right)^2$, where $u = l/2 \left(\pm \omega_d T - \frac{2\pi}{\lambda_L} y'' l \right)$. It is well known that $\left(\frac{\sin Nu}{\sin u} \right)^2$ has the following special characteristics:

when [i] $u = k\pi$, $k = 0, \pm 1, \pm 2, \dots$ maximum occurs

$$\lim_{u \rightarrow k\pi} \left(\frac{\sin Nu}{\sin u} \right)^2 = N^2$$

[ii] when $\sin u \neq 0, \sin Nu = 0$ minimum occurs

Minimum occurs at $Nu = \pi, 2\pi, \dots, (N-1)\pi, (N+1)\pi$

From [i] we know that the reconstructed images have maximum intensities at

$$\pm \omega_d T - \frac{2\pi y'' l}{\lambda_L} = 2k\pi$$

$$y'' = \frac{\lambda_L}{l} \left[\pm \frac{\omega_d T}{2\pi} - k \right] \quad (25)$$

where (+) signs signify that the maxima of $I_1(x'', y'')$ and $I_{-1}(x'', y'')$ are moving along the $+y''$ and $-y''$ directions with distance proportional to the Doppler frequency $\omega_d/2\pi$ (Hz)

From (25) it can be understood that corresponding to one target velocity (or a Doppler frequency) y'' has more than one value due to the presence of k . This is the cause of lack of clarity in velocity signals of a radar which is intrinsic to the radar system and still exists in the optical processing stage.

Based on [i], the lack of clarity should be the same and it should be proportional to N^2 . However, due to the presence of the factor $[(\sin 2\pi y''/F'\lambda_L \cdot m/2) \cdot 2\pi y''/F'\lambda_L]^2$ in equations (23) and (24), the corresponding intensity with each k value decreases along the y'' direction according to $(m/2)^2 (\sin W/W)^2$ and

$$W = 2\pi y''/F'\lambda_L \cdot m/2$$

which is determined by the width of each single hologram.

We also noted that the reconstructed signal of the combined hologram at $W=0$ is N^2 times more intense than that of a single hologram. This shows that multiple signals can drastically improve the signal to noise ratio using this holographic processing technique.

From property [ii] we may conclude that the first location for $\sin Nu/\sin u$ to be zero determines the width of the spectrum line. It is then possible to define the resolution of the Doppler frequency - velocity. Its first zero occurs at $Nu = \pi$ i.e.

$$\frac{N}{2} \frac{2\pi l}{F'\lambda_L} y'' = \pi$$

Therefore

$$y'' = \frac{F' \lambda'_L}{Nl} \Delta y''_{\min} \quad (26)$$

where $\Delta y''_{\min}$ is the spectrum line width or velocity resolution unit. For example, when $\lambda'_L = 0.6\mu$, $l = 120\mu$, $F' = 400$, $N = 50$, $\Delta y''_{\min} = 0.04$ or the spectrum line width is 0.04 mm in the y'' direction.

$$\Delta y''_{\min}$$

Plugging equation (26) into (25) we get

$$\Delta y''_{\min} = \frac{F' \lambda'_L}{l} (T \cdot f_{d\min})$$

$$f_{d\min} = \frac{l}{F' \lambda'_L} \frac{\Delta y''_{\min}}{T} = \frac{1}{NT} \text{ (Hz)}$$

where $f_{d\min}$ is the smallest unit of Doppler frequency resolvable in Hertz which is the same as the velocity resolution unit used in radar systems. For example, when $N = 50$ and $T = 200$ msec (corresponding to a repetition frequency $f_r = 1/T = 500$ Hz), $f_{d\min} = 10$ Hz.

III. Experiments and Results

The experimental set up of the holograms recording experiments is schematically shown in Figure 6. The pulse light from the laser is split into two beams. One shines directly on the reference beam ultrasonic light modulator and the other goes through a Fourier transform using a 400 mm focal length cylindrical lens. Interference occurs between the reference beam and the first order fringe and the hologram is recorded using a camera. The combined hologram is obtained by waving the film along the spectrum lines.

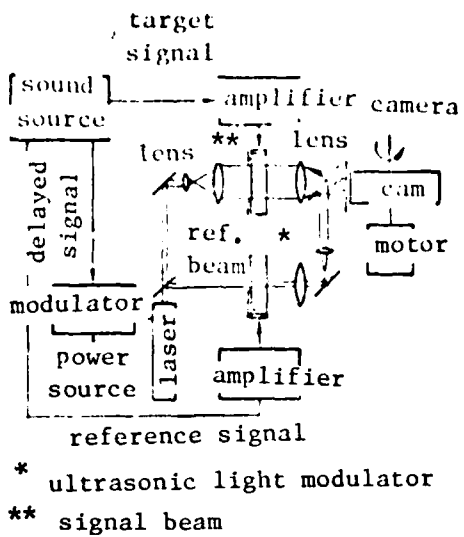


Figure 6. Two Dimensional Process System

1. Light Source

A pulse Xe laser at wavelength 5352.9\AA (which is suitable for the spectral response of the film) and bandwidth $0.5 \mu\text{sec}$ is used. Under partial compensation conditions, it is capable of recording signals 10^{12} Hz wide. The relevant length is a few centimeters. The operating voltage is $10 \sim 20 \text{ Kv}$ with current pulses at $\approx 1000 \text{ A}$.

2. Ultrasonic Light Modulator

The energy converter is made with X quartz crystal, $89 \mu\text{m}$ in thickness with a frequency at $30.3 \times 10^{12} \text{ Hz}$. The electrode area is $20 \times 5 \text{ mm}^2$ for the signal modulator and $30 \times 3 \text{ mm}^2$ for the reference beam modulator. The delay medium is water in which the speed of sound $s = 1.5 \times 10^5 \text{ cm/sec}$. The optical aperture of the signal modulator is 3 cm with storage time $20 \mu\text{sec}$ which corresponds to a storage air space of 6000 m. The bandwidth of the ultrasonic light modulator is $2 \times 10^{12} \text{ Hz}$. The signal modulator uses Debye diffraction, i.e. incident beam is parallel to the ultrasonic wave. The reference beam modulator is driven by continuous pulse signals using Bragg diffraction, which concentrates the diffracted beam on one spectral line to assure that the reference beam is always more intense than the signal beam.

3. Generating of the Reference Beam

The reference beam after passing through two short focal length cylindrical lenses is incident on the film at an angle in the form of a parallel beam. It has the same frequency as the signal beam.

4. Signal Source

Target signals and reference signals are generated by crystal oscillation. They are then amplified and sent to the energy converter. The target signal is generated by three crystals using their intrinsic frequency difference as the Doppler frequency. Four oscillating signals are generated by the pulse modulator with two signals of same frequency to simulate identical target velocity. The total length of the four signals is $< 20 \mu\text{m}$ with pulsing time $\sim 1 \mu\text{sec}$. Upon receiving the four signals into the modulator, a feedback pulse is synchronized with the laser pulses. The repetition frequency is 500 Hz.

5. Recording Medium and Driving Device

The recording medium is 35 mm film. Its resolution is approximately 200 lines/mm. In order to ensure a reasonable resolution $\geq \lambda_s$, the incidence angle is kept at less than 7° for $\lambda_L = 0.5 \mu\text{m}$ light ($\approx \sin\alpha = \lambda_L/\lambda_s$).

The film is loaded inside the camera with its cam driven by an electric motor at 0.16 rpm. There is a 120μ distance immediately next to the surface of the film (which is the width of the hologram). Each hologram is less than 5mm long. The results of the simulated signal experiments are shown in Figure 7 which displays the distance-velocity relationship of four targets in a two dimensional manner. Two of the targets have the same velocity. It is evident by the multiple display of target sig-

nals along the y" axis in Figure 7. This is due to the lack of clarity discussed before. The spacing corresponds to the repetition frequency, i.e. 500 Hz.

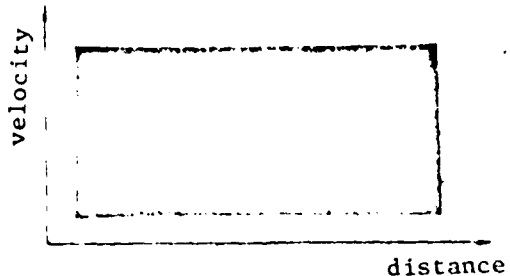


Figure 7. Two Dimensional Distance-Velocity Displays of 4 targets.

IV Discussion

The processing of two dimensional distance-velocity signals for multiple targets is becoming an important topic in modern radar system development. The electronic systems used to date (including computers) can only process one variable. Computers with parallel processing capabilities are still under development. Therefore, because of the limitation imposed by capacity and speed, complicated instruments are needed to realize the two dimensional processing of signals using methods which in principle are feasible. Holographic processing techniques appear to be far more attractive than those electronic methods based on capacity, speed, and capital equipment considerations.

This paper introduced the principles and experimental results of this holographic processing technique. It is our opinion that this technique has still a lot more potential to be further developed. For example its method is capable of processing pulse coded radar signals. This code design contains a function which is capable of increasing the clarity problem due to velocity. Based on this technique, the radar emits a series of coded pulse signal and the hologram of the returns is recorded using the ultrasonic light modulator. The difference is that

the holograms are no longer spaced equally by λ (See Figure 4). Instead, the i^{th} hologram is located $l_i = t_i^0 u$ away from the first one; when t_i^0 is the time at which the i^{th} pulse is transmitted and u is the linear velocity of the film. Therefore, the combined hologram is formed by these coded holograms. The light intensity distribution $I(y'')$ can then be expressed as:

$$I(y'') = \left(\frac{\sin \pi \frac{m}{F'\lambda_L} y''}{\frac{\pi y''}{F'\lambda_L}} \right)^2 \cdot \Sigma_0(y'') \quad (27)$$

$$\Sigma_0(y'') = \left| \sum_{k=1}^{50} e^{-j2\pi t_k^0 \left(\frac{u}{F'\lambda_L} y'' - t_k \right)} \right|^2 \quad (28)$$

where t_N^0 is the time at which the series of pulses is transmitted. The maximum of $\Sigma_0(y'')$ is located at:

$$y''_{\max} = \frac{F'\lambda_L'}{u} f_d = \frac{F'\lambda_L'}{l} \cdot \frac{\omega_d T}{2\pi} \quad (29)$$

which is proportional to the Doppler frequency, similar to what we found for equally spaced pulses as shown by (25). It is necessary to choose a suitable t_N^0 ($N=1 \dots 50$) value to make the $I(y'')$ distribution appear like a thumb-tag shape with a maximum at $y'' = y''_{\max}$, proportional to the Doppler frequency, to alleviate our velocity smearing problem without affecting the detection of velocity.

We designed several groups of coded pulse series and each contained 50 pulses. Table 1 shows one of the series studies. The pulses are separated by 2 - 20 msec with accuracy within 0.1 msec. The average space between pulses is 6-7 msec. Figure 8 shows the optical intensity distribution along the y'' axis when $f_d = 100$ and 300 Hz using an electronic computer to carry out the calculation. It is clearly demonstrated that the holographic processing of coded pulse signals is feasible.

Table 1. A Series of 50 Coded Pulses
(each pulse begins at t_N^o (sec.))

| Pulse No. | t_N^o |
|-----------|---------|-----------|---------|-----------|---------|-----------|---------|
| 1 | 0.0066 | 14 | 0.0819 | 27 | 0.1734 | 40 | 0.2844 |
| 2 | 0.0156 | 15 | 0.0917 | 28 | 0.1820 | 41 | 0.2939 |
| 3 | 0.0201 | 16 | 0.0942 | 29 | 0.1841 | 42 | 0.3013 |
| 4 | 0.0246 | 17 | 0.0989 | 30 | 0.2034 | 43 | 0.3042 |
| 5 | 0.0321 | 18 | 0.1014 | 31 | 0.2107 | 44 | 0.3095 |
| 6 | 0.0402 | 19 | 0.1195 | 32 | 0.3151 | 45 | 0.3189 |
| 7 | 0.0451 | 20 | 0.1260 | 33 | 0.2253 | 46 | 0.3247 |
| 8 | 0.0435 | 21 | 0.1337 | 34 | 0.2344 | 47 | 0.3344 |
| 9 | 0.0569 | 22 | 0.1360 | 35 | 0.2416 | 48 | 0.3438 |
| 10 | 0.0610 | 23 | 0.1538 | 36 | 0.2580 | 49 | 0.3492 |
| 11 | 0.0631 | 24 | 0.1601 | 37 | 0.2640 | 50 | 0.3581 |
| 12 | 0.0632 | 25 | 0.1657 | 38 | 0.2737 | | |
| 13 | 0.0710 | 26 | 0.1699 | 39 | 0.2804 | | |

Finally we must point out that although we limited our discussions to the processing of electrical radar signals using this holographic technique, this two dimensional display method may be applied to analyze data obtained in geological survey and sonar systems.

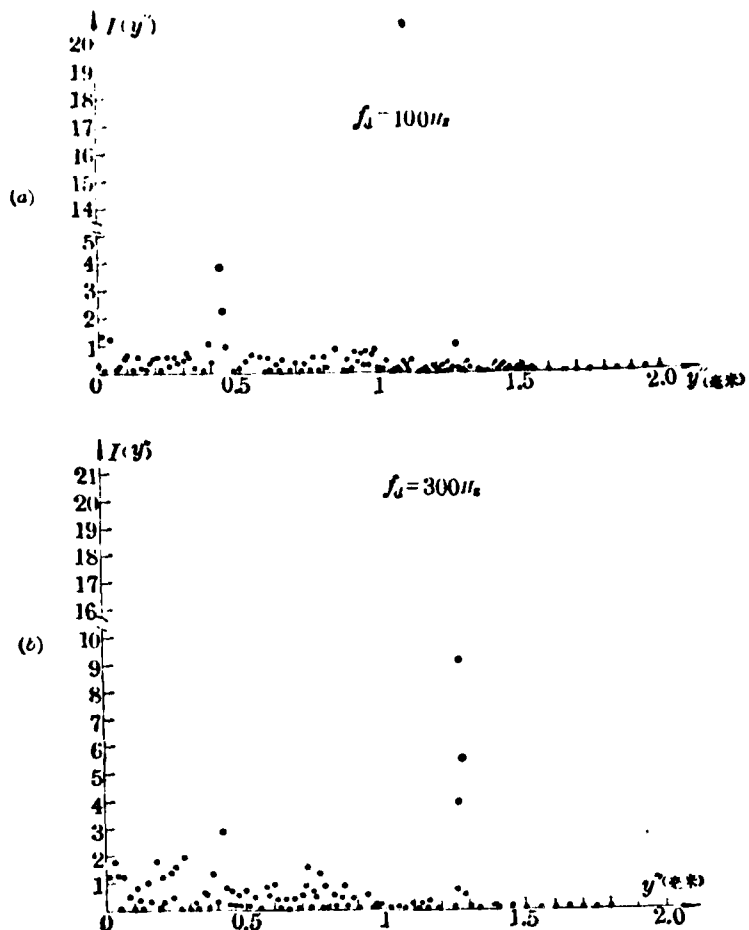


Figure 8.

References

- [1] M. Arm, M. King, *Appl. Opt.*, **8**, No. 7, 1413 (1969).
- [2] *Microwave*, **8**, No. 7, 26, 85 (1969). M. King, M. Arm; *IEEE J. Q. E.*, **QE 5**, No. 6, 332 (1969).
- [3] A. Vander Lugt; *IEEE Trans. Information Theory*, **IT-10**, 139 (1964).
- [4] F. E. Nathanson; *Radar design principles* §11.3